International Immunology, Vol. 11, No. 5, pp. 777–786

T cell activation-associated epitopes of CD147 in regulation of the T cell response, and their definition by antibody affinity and antigen density

Christian Koch, Gunther Staffler, Robert Hüttinger, Ivan Hilgert[1], Elisabeth Prager, Jan Cerny[1,2], Peter Steinlein[3], Otto Majdic, Václav Horejší[1] and **Hannes Stockinger**

Institute of Immunology–Vienna International Research Cooperation Center at NFI, University of Vienna, Brunner Strasse 59, 1235 Vienna, Austria
[1]Institute of Molecular Genetics, Academy of Sciences of the Czech Republic, 142 20 Prague 4, Czech Republic
[2]Faculty of Sciences, Charles University, 142 20 Prague 4, Czech Republic
[3]Institute of Molecular Pathology, 1030 Vienna, Austria

Keywords: antibodies, cell surface molecules, human, T lymphocytes, signal transduction

Abstract

CD147 is a broadly expressed cell surface glycoprotein of the Ig superfamily whose expression is up-regulated upon T cell activation. In order to elucidate a possible role of CD147 in T cell biology, we established 15 specific mAb. Seven distinct epitopes were defined by the mAb panel. Most of the mAb bound only to phytohemagglutinin (PHA)-activated but not resting T cells. We demonstrate that this was not because of true expression of activation-dependent neoepitopes but rather due to bivalent binding of the relatively low-affinity mAb (affinity constant K_A values between 2.25×10^8 and 7×10^9 M^{-1}) to the more densely expressed and/or more clustered CD147 molecules on the activated T cells. In contrast, the mAb with higher affinity ($K_A > 7 \times 10^9$ M^{-1}) could stably bind in a monovalent fashion even to the relatively low dense CD147 molecules on resting T cells. This model might more generally explain the nature of 'activation epitopes' described previously in other leukocyte surface molecules. Finally, we provide evidence that induction of ordered dimerization of CD147 by a mAb directed to a unique epitope results in strong inhibition of CD3-mediated T cell activation.

Introduction

The human cell surface molecule CD147 was designated at the Sixth International Workshop and Conference of Human Leukocyte Differentiation Antigens (1). It is a glycoprotein of 50–60 kDa having typical features of a type I integral membrane protein of the Ig superfamily. CD147 is also known as M6 antigen (2), extracellular matrix metalloproteinase inducer (EMMPRIN) (3) or human basigin (4). In various species glycoproteins homologous to CD147 have been identified, i.e. the rat protein OX-47/CE9 (5–7), the chicken blood–brain barrier-related molecule HT7/neurothelin/5A11 (8–10), the mouse protein gp42/basigin (11,12) and the rabbit homologue (13).

The CD147 molecule is broadly expressed on human peripheral blood cells, endothelial cells, and cultured cells of hemopoietic and non-hemopoietic origin (1). In T cells, its expression level is dependent on the differentiation state. Thymocytes are more strongly positive than mature T cells (14) and phytohemagglutinin (PHA)-activated T blasts express increased levels of CD147 (2). Significant expression of CD147 has also been reported in neoplasms of the bladder, liver and lung (15,16).

The molecular function of neither CD147 nor any of its species homologues is fully understood. However, one can suggest that CD147 is involved in signal transduction and cell adhesion functioning either directly as a signal transmitting adhesion molecule or as a regulator of adhesion. Upon interaction with fibroblasts, it seems to be responsible for the induction of expression of the matrix metalloproteases interstitial collagenase, gelatinase A and stromelysin-1, therefore the term EMMPRIN (3,17); certain CD147 mAb were reported to inhibit

The first two authors contributed equally to this work

Correspondence to: H. Stockinger

Transmitting editor: I. Pecht

Received 8 December 1998, *accepted* 29 January 1999

homotypic aggregation of the estrogen-dependent breast cancer cell line MCF-7, as well as MCF-7 cell adhesion to type IV collagen, fibronectin and laminin (18); a mAb to the chicken homologue reduced retina cell aggregation (10). Furthermore, CD147 was recently found to co-immunoprecipitate with $\alpha_3\beta_1$ and $\alpha_6\beta_1$ integrins, and to co-localize with these integrins in areas of cell–cell contact (19).

Mice lacking the mouse homologue exhibit infertility of both sexes (20,21), seem to have an abnormality in reception of odor (22), and show a worse performance in short-term memory and latent learning (23). Moreover, lymphocytes of such mice give an enhanced mixed lymphocyte reaction (22). Together, these studies indicate a significant role of CD147 in reproduction, functioning of the neuronal system and regulation of the immune system.

The aim of this study was to provide a more detailed molecular and functional characterization of the CD147 molecule in the human immune system. For this purpose, we established a panel of new CD147 mAb. We identified seven mAb-defined epitopes and demonstrated that the binding of T cell activation-restricted mAb is not dependent on *de novo* T cell epitope expression, but on mAb affinity and antigen density and/or clustering. Finally, by using a unique CD147 mAb we provide evidence that CD147 is involved in regulation of the T cell response.

Methods

Construction and expression of soluble recombinant CD147 proteins

A CDM8-derived receptor globulin (Rg) expression plasmid encoding soluble recombinant CD2Rg, i.e. the extracellular domain of CD2 fused to the DNA coding for the hinge region, C_H2- and C_H3 domain of human IgG1, was kindly provided by Dr B. Seed (Department of Molecular Biology, Massachusetts General Hospital, Boston, MA). Soluble recombinant CD147Rg was constructed in the Rg expression plasmid essentially as described (24) by replacing the extracellular domain sequence of CD2 by that of CD147, which was amplified by PCR from the CD147 plasmid H34 (2). CD147Rg/D1 and CD147Rg/D2 containing either the membrane-distal (D1) or the membrane-proximal domain (D2) of CD147 were established by the same approach.

For production of the chimeric molecules, the expression plasmids were co-transfected with a selectable marker plasmid, pSV2-dhfr (25), into dihydrofolate reductase-deficient CHO cells (CHO *dhfr*$^-$) according to Chen and Okayama (26). Alternatively, the gene constructs were inserted into the plasmid pXMT3 which confers stable maintenance of genes in CHO *dhfr*$^-$ cells. Supernatants of transformed colonies were assayed for the presence of soluble fusion proteins by ELISA or by using the fluorimetric bead assay described below. Positive transfectants were subcloned by limiting dilution and then passaged by increasing the concentration of methotrexate to a final level of 1 μM. Transformants producing high levels of the chimeric molecules were expanded in serum-free Ultraculture medium (Whittaker Bioproducts, Walkersville, MD). CD147Rg was purified from the supernatants using a Protein A-CR column (BioProcessing, Consett, UK).

Monomeric soluble CD147–StrepTag (ST) fusion proteins were constructed by replacing the DNA coding for the constant parts of human IgG1 in CD147Rg by the DNA coding for ST which was derived from vector pASK60 (27). For the generation of dimeric ST constructs, the hinge region of human IgG1 was inserted between the cDNAs encoding the extracellular region of CD147 and ST. The resulting soluble dimeric forms of CD147 were termed CD147-hinge–StrepTag (CD147-H–ST).

Preparation of mAb

BALB/c mice were repeatedly immunized with CD147Rg in complete Freund's adjuvant and 4 days after the final i.v. boost immunization, the spleen cells were fused with Sp2/0 myeloma cells. The hybridomas secreting CD147-specific mAb were selected by the microfluorimetric bead assay (see below) using beads coated with CD147Rg. CD31Rg (28)-coated beads were used as negative control.

Analysis of CD147 mAb binding by using BIAcore

All measurements were performed on the BIAcore biosensor instrument (Pharmacia Biosensor, Uppsala, Sweden). The sensor chip was coated with a donkey $F(ab')_2$ anti-human IgG antibody (Jackson ImmunoResearch, West Grove, PA) according to the standard procedures (29). The immobilization of CD147Rg and the mAb binding analysis on immobilized CD147Rg were performed at 25°C with HEPES-buffered saline (HBS) (10 mM HEPES, pH 7.3, 150 mM NaCl, 3.4 mM EDTA and 0.05% Surfactant P20) as continuous flow buffer at a constant flow rate of 5 μl/min.

For the epitope mapping analysis, 20 μl of CD147Rg (diluted to 40 μg/ml in HBS buffer) was injected followed by 10 μl of the first mAb at a concentration of 10 μg/ml and 10 μl of the second mAb at the same concentration.

For the kinetic analysis, 35 μl of the mAb solutions was injected over a total time of 7 min for determination of the association phase. The dissociation phase was monitored over a period of 15 min. Three cycles with different concentrations (3, 6 and 25 nM) of the mAb were used for evaluation. The analysis of the association and dissociation phases was performed with BIAevaluation version 3.0 software, which allows simultaneous evaluation of the kinetic constants of the association and dissociation phases.

Microfluorimetric bead assay

Immunobeads coated with rabbit anti-human IgG antibodies (1×10^9/ml; Irvine Scientific, Santa Ana, CA) were incubated with supernatants of transfectants expressing the different Rg constructs at 37°C. After blocking with human IgG (100 μg/ml) in PBS for 20 min at 4°C, Rg-loaded immunobeads (1×10^5) were stained by an indirect immunofluorescence technique using mAb and FITC-conjugated sheep $F(ab')_2$ anti-mouse IgG + IgM antibodies (An der Grub, Vienna, Austria). Fluorescence was analyzed on a FACScan (Becton Dickinson, Mountain View, CA) flow cytometer.

To analyze the binding capacity of the CD147 mAb to the monomeric or dimeric StrepTagged CD147 constructs, immunobeads coated with rabbit anti-mouse IgG antibodies (1×10^9/ml; Irvine Scientific) were loaded with the respective CD147 mAb and then incubated with supernatants of transfec-

tants expressing either CD147–ST or CD147-H–ST. Binding of the soluble CD147 molecules was detected by phycoerythrin-conjugated streptavidin (Becton Dickinson) and flow cytometry.

T cell activation and proliferation assays

Peripheral blood mononuclear cells (PBMC) were isolated from blood of healthy donors by standard density-gradient centrifugation using Ficoll-Hypaque (Pharmacia, Uppsala, Sweden). T cells were separated by nylon wool, and subsequent removal of $CD14^+$, $CD16^+$, $CD20^+$ and $CD56^+$ cells by magnetic sorting using the MACS technique (Miltenyi Biotech, Bergisch Gladbach, Germany). As determined by CD3 staining, the resulting cell population contained >98% T cells. To analyze the influence of the CD147 mAb on T cell proliferation, T cells (5×10^4 cells/well) were seeded in 96-well flat-bottom tissue culture plates (Nunc, Roskilde, Denmark) and CD3 mAb OKT3 (1 μg/ml, Ortho Pharmaceuticals, Raritan, NJ) and CD147 mAb (at concentrations indicated) were added simultaneously. Alternatively, 96-well flat-bottom plates were coated overnight at 4°C with 100 μl of CD147 mAb diluted in PBS (at concentrations indicated) followed by washing the plates twice with PBS. After blocking free binding sites by incubation with RPMI 1640 plus 10% FCS at 37°C for 1 h, 5×10^4 T cells were added per well plus OKT3 (1 μg/ml). After 72 h of incubation, proliferation was determined by quantitating [^{3}H]thymidine (1 μCi/well) incorporation during the last 18 h of culture. For immunofluorimetric analysis of CD147 mAb binding, PBMC were stimulated for 3 days with 0.01 U/ml PHA (Wellcome, Beckham, UK) in RPMI 1640 medium supplemented with 10% FCS and 2 mM L-glutamine.

Immunofluorescence analysis

Freshly isolated peripheral blood T cells or PHA-activated T blasts (5×10^6/ml) were incubated with mAb (10 μg/ml) in PBS containing 1% BSA and 0.02% NaN_3 for 30 min at 4°C. After washing, cells were stained for 30 min at 4°C with FITC-conjugated sheep $F(ab')_2$ anti-mouse IgG + IgM antibodies (An der Grub). To prevent non-specific binding of mAb, the cells were preincubated for 30 min at 4°C with 4 mg/ml of human Ig. Fluorescence was analyzed on a FACScan flow cytometer (Becton Dickinson). Dead cells were excluded from the analysis by DNA staining with ethidium bromide.

Western blotting and gel filtration of cell lysates

For Western blotting, cells were lysed in PBS, pH 7.0, containing 1% NP-40 detergent (Pierce, Rockford, IL), and the protease inhibitors iodoacetamide (5 mM), aprotinin (5 mM), leupeptin (5 mM), PMSF (1 mM) and pepstatin (1 mM; all from Sigma, St Louis, MO). After incubation for 30 min on ice, nuclei were removed by centrifugation at 10,000 *g* for 10 min at 4°C. The lysates were resolved on a 8% SDS–PAGE gel and transferred to an Immobilon-P membrane (Millipore, Bedford, MA). After a 40 min incubation in blocking buffer [Tris-buffered saline (TBS), pH 7.5, containing 4% non-fat powdered milk], blots were probed with the indicated mAb for 40 min, washed in TBS/0.1% Tween 20 and incubated for 30 min with horseradish peroxidase-conjugated goat anti-mouse IgG (BioRad, Richmond, CA). Proteins were visualized by an enhanced chemiluminescence detection system (Boehringer Mannheim, Mannheim, Germany) and a Lumi-Imager (Boehringer Mannheim).

To investigate activation-induced clustering of CD147 molecules, 5×10^7 freshly isolated peripheral blood T cells or PHA-activated (5 days) T blasts were solubilized in ice-cold lysis buffer (0.15 M NaCl, 0.1 M Tris–HCl, pH 8.2, 1% laurylmaltoside as detergent, and the protease inhibitors 1 mM Pefabloc and 5 mM iodoacetamide). Nuclei and other insoluble materials were removed by low-speed centrifugation (3000 *g*, 5 min). The supernatant was fractionated by gel filtration on a 1 ml minicolumn of Sepharose 4B as described elsewhere (30) and 0.1 ml fractions were analyzed by non-reducing SDS–PAGE followed by Western blotting. The column was calibrated by size standards; the void volume corresponded to fractions 3–4, maxima of IgM (900 kDa) and IgG (160 kDa) were eluted in fractions 6 and 8 respectively.

Results

Preparation of novel CD147 mAb

To establish a panel of new CD147 mAb we specifically immunized mice with a soluble recombinant form of CD147, CD147Rg, which consists of the cDNA coding for the entire extracellular region of CD147 fused to the DNA coding for the hinge region, C_H2- and C_H3 domain of human IgG1. Due to the disulfide bonds of the hinge region, CD147Rg is (like antibodies) secreted by transfectants as a dimer (see Methods). CD147 mAb-producing hybridomas were screened by a highly sensitive microfluorimetric bead assay (31), i.e. immunofluorescence staining and flow cytometric analysis of beads coated with CD147Rg. Using this approach, 13 mAb, named MEM-M6/1–MEM-M6/13, were prepared which specifically reacted with the CD147Rg-coated beads (data not shown, *cf.* Fig. 3).

Western blotting analysis confirmed the specificity of these mAb (Fig. 1). mAb MEM-M6/1, MEM-M6/2, MEM-M6/3, MEM-M6/4, MEM-M6/6, MEM-M6/10 and MEM-M6/13 stained a dominant zone of ~45–60 kDa. A band in that range appeared also in the immunoblots of MEM-M6/9 and MEM-M6/11. A

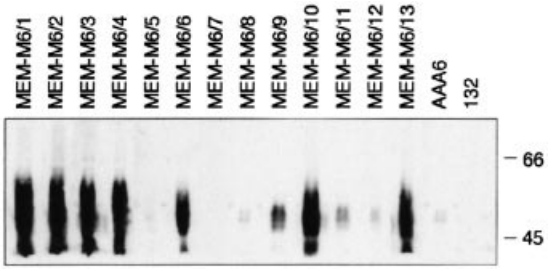

Fig. 1. Analysis of the newly established CD147 mAb by Western blotting. Lysates of human fibroblastoid 293 cells were separated by SDS–PAGE under non-reducing conditions. After transfer to a nitrocellulose membrane, the blot was incubated with the indicated CD147 mAb, and developed by using an anti-mouse horseradish peroxidase conjugate and the enhanced chemiluminescence detection system of Boehringer Mannheim. Only the relevant part of the blot is shown. Molecular mass markers are indicated in kDa.

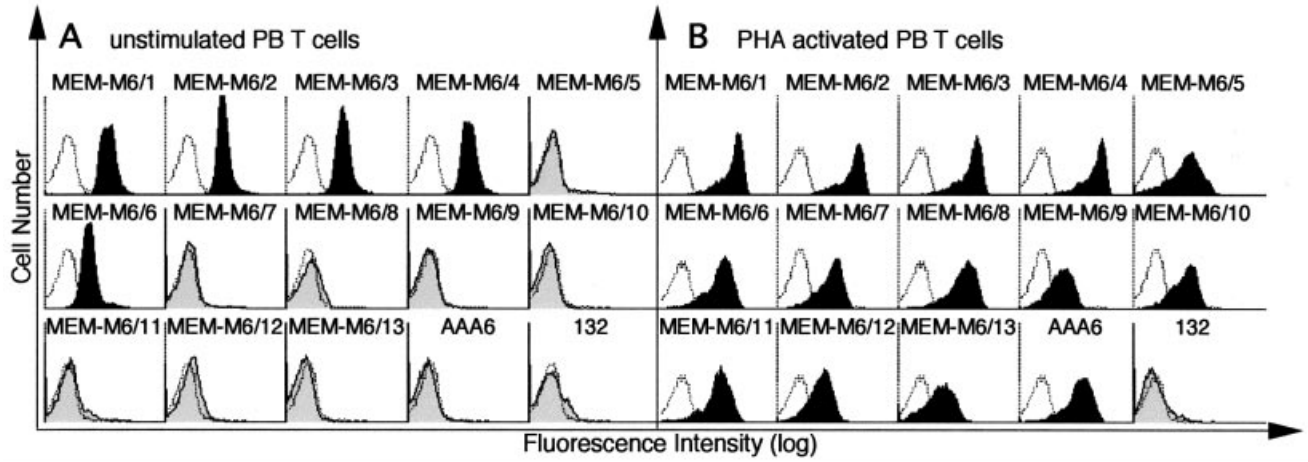

Fig. 2. FACS staining profiles of the CD147 mAb with unstimulated (A) and PHA-activated (B) peripheral blood (PB) T cells. The reactivity of the control mAb is overlaid (dotted histograms).

similar band, though with much weaker intensity, was found with MEM-M6/8, MEM-M6/12 and CD147 reference mAb AAA6 that was generated earlier in our Institute (2).

We never obtained positive results by Western blotting or immunoprecipitation with mAb MEM-M6/5, MEM-M6/7 and 132, the latter was generated also earlier (32). In addition to binding to CD147Rg, these mAb specifically reacted with a variety of CD147 transfectants including monkey COS cells, mouse NIH-3T3 and BW5147 cells, as well as chicken HD3 cells (data not shown).

Cellular reactivity of the CD147 mAb

Earlier studies performed with the CD147 mAb AAA6 (2) and 8D6 (14) as well as with the CD147 mAb that were identified at the Sixth International Workshop on Human Leukocyte Differentiation Antigens (1) revealed a broad expression of CD147 on hemopoietic and non-hemopoietic cells. We evaluated the binding capacity of the new panel of mAb on a variety of cell lines including the T cell lines HPB-ALL and HUT78, the B cell line NALM6, the ovarian carcinoma cell line OV-MZ6, and the estrogen-dependent breast cancer cell line MCF7. All 13 novel mAb were positive, and displayed a similar FACS staining profile as the mAb 132 and the reference mAb AAA6 (data not shown).

Flow cytometric analysis of PBMC subdivided the mAb into three groups. Whereas all of the mAb stained monocytes (data not shown), a clear difference was observed with T lymphocytes. While mAb MEM-M6/1, MEM-M6/2, MEM-M6/3, MEM-M6/4 and MEM-M6/6 reacted with T cells, no significant binding was observed with mAb MEM-M6/5, MEM-M6/8, MEM-M6/9, MEM-M6/10, MEM-M6/11, MEM-M6/12, MEM-M6/13 and AAA6. However, the latter mAb bound T cells activated for 3 days with PHA. One mAb, 132, stained neither resting nor activated T cells (Fig. 2).

Furthermore, T cell activation increased the staining intensity of those mAb which recognized unstimulated T cells (Fig. 2). These data corroborated that CD147 is a T cell activation-associated surface antigen (2) and suggested, at first glance, that expression of some mAb-defined CD147 epitopes is activation dependent. Given the functional significance of certain T cell activation-associated epitopes (33), we set out to analyze the molecular events underlying their expression.

Reactivity of the CD147 mAb with the individual Ig domains of the CD147 molecule

In a first set of experiments, we localized the mAb-defined determinants to the individual Ig domains of the CD147 molecule. We constructed and produced truncated forms of CD147Rg, CD147Rg/D1 and CD147Rg/D2, which contained instead of the entire extracellular region, either the N-terminal (D1) or membrane proximal (D2) Ig domain of CD147. Staining of beads coated with these constructs revealed mAb MEM-M6/1, MEM-M6/2, MEM-M6/3, MEM-M6/4, MEM-M6/5, MEM-M6/8, MEM-M6/9, MEM-M6/10, MEM-M6/11, MEM-M6/13, AAA6 and 132 as specific for the Ig domain D1, and mAb MEM-M6/6, MEM-M6/7 and MEM-M6/12 as reactive with the Ig domain D2 of CD147 (Fig. 3). Since this reactivity did not correlate with the mAb grouping obtained by staining T lymphocytes (Fig. 2), we subsequently performed a detailed epitope mapping by mAb cross-blocking analysis.

Epitope mapping analysis

Real-time biospecific interaction analysis (BIAcore) was used for epitope mapping analyses. We investigated the ability of individual CD147 mAb to influence the binding of the others to the CD147 molecule. CD147Rg was bound to the dextran matrix of the BIAcore sensor chip surface (via its Fc fragment to immobilized donkey anti-human antibody) and solutions of the 15 CD147 mAb were injected in pairs. Pairs of mAb, e.g. MEM-M6/1 followed by MEM-M6/6, were injected also in reverse order (MEM-M6/6 followed by MEM-M6/1). The only exceptions were extremely low-affinity mAb. Due to the high dissociation rate constants (k_d) of these mAb, i.e. mAb MEM-M6/5, AAA6 and 132, $k_d = >4.00\times10^{-3}$ s^{-1} (see Table 1), they were only used as second-step reagents (Fig. 4).

A complete overview of the cross-blocking analysis is shown in the reactivity matrix in Fig. 5. For example, binding

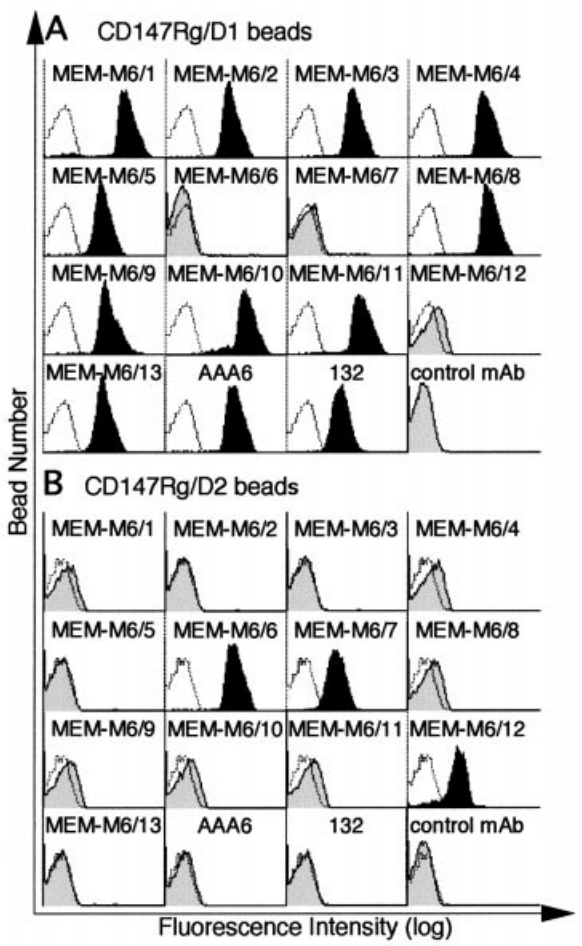

Fig. 3. Reactivity of the CD147 mAb with the N-terminal (D1) and the membrane-proximal (D2) Ig domain of CD147. Immunobeads coated with rabbit anti-human antibody were loaded with Rg consisting either of D1 (CD147Rg/D1) or D2 (CD147Rg/D2) of CD147. The beads were immunostained by using the individual CD147 mAb and analyzed by flow cytometry. The reactivity of the control mAb is overlaid (dotted histograms).

of mAb MEM-M6/1 inhibits binding of itself and of the mAb MEM-M6/2, MEM-M6/11 and 132 (indicated by gray circles); binding of all the other mAb to CD147 is not influenced (indicated by black circles). The same pattern was found with mAb MEM-M6/2 and 132 but not with MEM-M6/11. Thus, mAb MEM-M6/1, MEM-M6/2 and 132 were grouped together. In summary, the 15 CD147 mAb were clustered into seven major groups defining seven putative epitopes which are summarized in Fig. 6. Each hexagon represents an individual epitope family. Cross-inhibition of mAb of one epitope with mAb of another epitope suggested a sterical/spatial relationship of the epitopes which is indicated by overlapping sides in the two-dimensional epitope map. In detail, binding of mAb MEM-M6/11 inhibited and was inhibited by mAb of group 2, 3 and 6. Thus, binding of this mAb blocked the majority of the other CD147 mAb and vice versa suggesting that MEM-M6/11 recognizes a central epitope, which was therefore termed epitope 1. Similarly, group 2 mAb, i.e. MEM-M6/5, MEM-M6/8, MEM-M6/9, MEM-M6/10 and MEM-M6/13, mutu-

Table 1. Kinetic rate constants of CD147 mAb[a]

mAb	k_a[b]	k_d[c]	k_A[d]	k_D[e]
MEM-M6/3	2.12×10^6	7.44×10^{-5}	2.85×10^{10}	3.51×10^{-11}
MEM-M6/1	1.08×10^6	5.66×10^{-5}	1.91×10^{10}	5.24×10^{-11}
MEM-M6/4	1.63×10^6	1.09×10^{-4}	1.50×10^{10}	6.69×10^{-11}
MEM-M6/2	5.21×10^5	7.00×10^{-5}	7.44×10^9	1.34×10^{-10}
MEM-M6/6	3.60×10^5	4.94×10^{-5}	7.29×10^9	1.37×10^{-10}
MEM-M6/8	1.25×10^6	6.72×10^{-4}	1.86×10^9	5.38×10^{-10}
MEM-M6/10	1.57×10^5	1.10×10^{-4}	1.43×10^9	7.01×10^{-10}
MEM-M6/12	2.55×10^5	1.82×10^{-4}	1.40×10^9	7.14×10^{-10}
MEM-M6/7	2.75×10^5	2.01×10^{-4}	1.37×10^9	7.31×10^{-10}
MEM-M6/9	4.73×10^4	7.20×10^{-5}	6.57×10^8	1.52×10^{-9}
MEM-M6/5	1.16×10^6	2.26×10^{-3}	5.13×10^8	1.95×10^{-9}
MEM-M6/13	1.61×10^5	3.34×10^{-4}	4.82×10^8	2.07×10^{-9}
AAA6	7.13×10^5	1.64×10^{-3}	4.35×10^8	2.30×10^{-9}
MEM-M6/11	1.10×10^5	4.88×10^{-4}	2.25×10^8	4.44×10^{-9}
132	8.14×10^5	3.71×10^{-3}	2.19×10^8	4.56×10^{-9}

[a]Kinetic rate constants of CD14 mAb to CD147Rg evaluated by using the BIAevaluation program.
[b]k_a association rate constant (M^{-1} s^{-1}).
[c]k_d dissociation rate constant (s^{-1}).
[d]K_A equilibrium binding (affinity) constant (M^{-1}).
[e]K_D equilibrium dissociation constant (M).

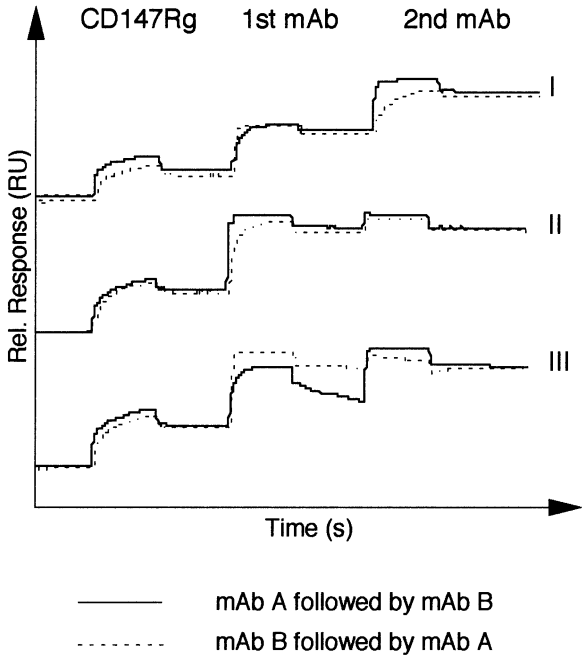

Fig. 4. Epitope mapping of the CD147 mAb by cross-blocking analysis using BIAcore. The surface of the BIAcore sensor chip was modified by covalent immobilization of a donkey anti-human antibody to allow the binding of CD147Rg to the sensor. Binding of CD147Rg and of the mAb caused a change of mass on the sensor surface which is displayed in relative RU. Pairs of mAb (A followed by B) were also injected in reverse order (B followed by A) to ensure the results of the cross-blocking analysis. Due to their high k_d, some low-affinity mAb could only be tested when injected as second-step reagents. The sensorgrams of the mAb MEM-M6/1 (A) and MEM-M6/6 (B) are shown as an example for simultaneous binding (I), those of the mAb MEM-M6/3 (A) and MEM-M6/4 (B) for inhibition of binding (II) and those of the mAb MEM-M6/5 (A) and MEM-M6/4 (B) when one mAb (MEM-M6/5) has a high k_d (III).

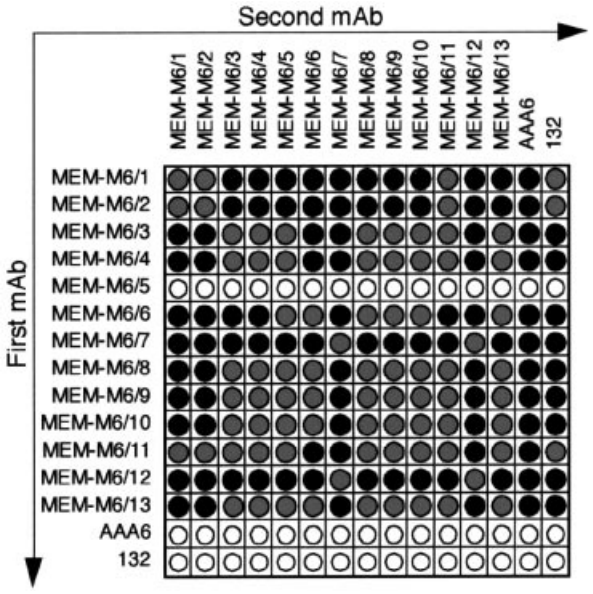

Fig. 5. The reactivity matrix of the cross-blocking analysis. ● Pairs of mAb which bind simultaneously; ◍ pairs of mAb which inhibit binding of each other; ○ pairs of mAb which have not been tested because of the high k_d of the first mAb.

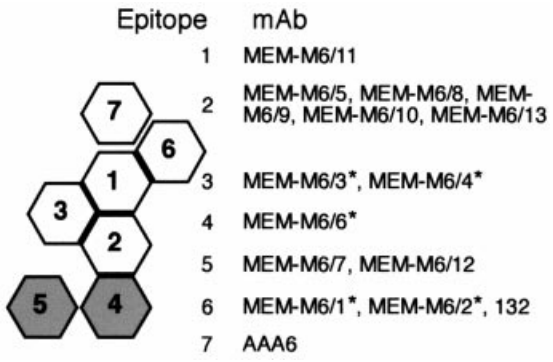

Fig. 6. Relation of the CD147 epitopes. Each hexagon represents one epitope. The mutual inhibition of mAb from different epitopes is indicated by overlapping sides. White hexagons represent epitopes in the N-terminal Ig domain (D1) of CD147, gray hexagons epitopes in the membrane proximal Ig domain (D2). mAb marked with an asterisk bind to unstimulated peripheral blood T cells.

ally inhibited each other as well as group 1, 3 and 4 mAb, suggesting that they also recognize an inner determinant, designated epitope 2. Epitope 3 is recognized by mAb MEM-M6/3 and MEM-M6/4, which were mutually inhibited by epitope 1 and 2 mAb. Epitope 4 is seen by MEM-M6/6 which was only cross-blocked by epitope 2 mAb. Epitope 5 is recognized by mAb MEM-M6/7 and MEM-M6/12, a pair of mAb which mutually inhibited each other but did not interfere with any other mAb. Group 6 consists of mAb MEM-M6/1, MEM-M6/2 and 132 which cross-inhibited epitope 1 mAb MEM-M6/11. AAA6, assigned as epitope 7 mAb, was not inhibited by any of the CD147 mAb in this study. However, the k_d of this mAb to the CD147 molecule was stabilized when epitope 6 mAb were pre-bound (data not shown).

When the epitope specificity of the CD147 mAb and their reactivity with resting T cells were compared, it appeared that epitopes 3 and 4 were exposed on resting T cells while the other epitopes appeared only upon T cell activation. Epitope 6 did not fit into this scheme: mAb MEM-M6/1 and MEM-M6/2 reacted with resting T cells, whereas mAb 132 did not display a significant binding both with resting and activated T cells (*cf.* Figs 2 and 5). In search for a molecular explanation of this phenomenon as well as of the activation-associated epitopes, we asked whether differences in the association and dissociation characteristics of the individual CD147 mAb which we observed during the epitope mapping analysis could play a role for the different staining patterns of the mAb.

Analysis of the association and dissociation constants of the CD147 mAb

For a detailed analysis of the association and dissociation constants of the mAb, we coated CD147Rg on the surface of the BIAcore sensor chip followed by injection of the individual CD147 mAb. To avoid mass transfer limitations, CD147Rg was loaded as low as possible [in the range of 100–130 resonance units (RU)] on the BIAcore sensor chip and CD147 mAb were injected at three different concentrations (3, 6 and 25 nM). To determine an appropriate model for evaluation of the kinetics, the binding capacity of the CD147 mAb was investigated. Due to the antibody-like structure of CD147Rg two possible mAb binding sites are present in one molecule. Indeed the calculation of the stoichiometric ratios between the CD147 mAb bound to CD147Rg revealed a 1:1 interaction (data not shown). Therefore, the association rate constant k_a, the dissociation rate constant k_d, the affinity constant K_A and the dissociation constant K_D of the CD147 mAb were calculated using the predefined Langmuir 1:1 interaction model provided in the BIAevaluation software package.

Comparison of the affinity constants K_A with the staining profiles of the mAb revealed that resting T cells reacted with those mAb that exhibited $K_A > 7\times10^9$ M^{-1} (mAb MEM-M6/1, MEM-M6/2, MEM-M6/3, MEM-M6/4 and MEM-M6/6) and, therefore, can be considered as mAb with a relative high affinity (Table 1). A plausible reason for the lack of staining of resting T cells by the low-affinity mAb was that they were washed away from the cells during the staining procedure. However, why are the lower-affinity mAb not similarly washed away from activated T cells (and from other blood cells and cell lines)? This difference is probably linked to different density of the CD147 molecule on the resting versus activated T cells. Three independent experiments showed that expression of CD147 is ~3 times higher upon T cell activation by PHA as indicated by mean fluorescence intensity values (MFI) of the high-affinity mAb MEM-M6/1 with activated T cells (MFI 205 ± 18) compared to resting T cells (MFI 61 ± 14) (Fig. 2). Thus, both the mAb affinity and the CD147 density appear to be important: at low antigen density only high-affinity mAb resist the staining procedure, because even their monovalent binding may be sufficiently stable (binding of the second antibody arm to a second antigen is not necessary and is also unlikely because of low density); in contrast, in the case of low-affinity mAb only bivalent binding, which requires as prerequisite two adjacent antigen molecules, may be strong

enough to survive the washing steps during the staining procedure. This situation may obviously occur at higher surface antigen density or if the antigen is unevenly distributed (clustered) on the cell surface. To prove this hypothesis, we investigated the binding characteristics of the CD147 mAb to monomeric and dimeric forms of CD147.

Binding of the CD147 mAb to monomeric and dimeric forms of CD147

For the generation of monomers and dimers of CD147, we replaced the hinge region, CH2 and CH3 domain of human IgG1 in the CD147Rg dimers by a smaller tag. We used ST, a hydrophilic peptide sequence of 10 amino acids, which is bound by streptavidin (27). The monomeric form, termed CD147–ST, was constructed by fusing ST C-terminal to the extracellular domain of CD147. For dimerization, we made use of the cysteine bonds of the human IgG1 hinge region which was inserted between the CD147 extracellular domain and ST resulting in dimeric CD147-H–ST molecules (see Methods).

To analyze the binding capacity of the CD147 mAb to monomers and dimers of CD147, the mAb were coated onto beads and these were then incubated with solutions containing the recombinant CD147 constructs in soluble form. Binding of the soluble ST–(H) fusion proteins by the mAb was visualized by a streptavidin–phycoerythrin conjugate and flow cytometry. As can be seen in Fig. 7, the monomeric forms of CD147 were only bound by those mAb which were able to stain resting T cells and possessed a relatively high affinity (i.e. MEM-M6/1, MEM-M6/2, MEM-M6/3, MEM-M6/4 and MEM-M6/6). In contrast, the dimeric forms were effectively immobilized by all mAb with the exception of mAb 132, a pattern which is identical to the staining of the mAb panel with PHA-activated T blasts. However, when incubation times of >2 h were allowed then mAb 132, which has the lowest affinity constant among the mAb ($K_A = 2.19\times10^8\,M^{-1}$), was also able to bind the dimeric CD147-H–ST. Under such a condition, 132 also stained PHA-activated T cells (data not shown). Together, this study strongly suggests that the activation-associated CD147 epitopes defined on T cells by our new mAb are determined by mAb affinity and antigen density, and not by *de novo* expression/exposure. The relatively high-affinity mAb can strongly bind in a stable way to the antigen in the monovalent fashion, whereas low-affinity mAb require bivalent binding to two adjacent antigens, a condition which seems to be fulfilled on activated T cells through CD147 up-regulation. In addition to or alternatively to antigen up-regulation, low-affinity mAb binding could be promoted through antigen clustering or multimerization. Indeed, a significant fraction of CD147 in PHA-activated as opposed to resting T cells appears to be present in very large complexes resistant to the mild detergent laurylmaltoside (Fig. 8). In this respect, it is of further interest that the 5A11/HT7 antigen, the avian homologue of CD147, was reported to form dimers and oligomers in certain cells (34).

Influence of the CD147 mAb on T cell activation

Finally, we examined a possible functional significance of the newly defined epitopes in T cell activation. We also further tested in this way the validity of the monovalent/bivalent

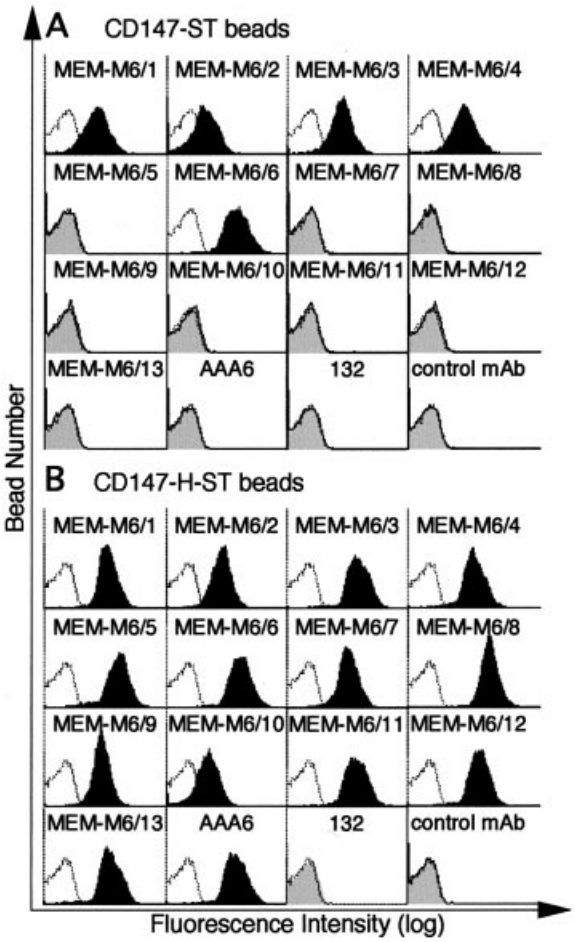

Fig. 7. Immobilization of monomeric CD147–ST and dimeric CD147-H–ST by CD147 mAb. The individual CD147 mAb were coated on rabbit anti-mouse beads which were then incubated with supernatants of transfectants containing either CD147–ST or CD147-H–ST. Binding of the ST fusion proteins by the mAb was detected by a streptavidin–phycoerythrin conjugate and flow cytometry. The profile obtained with the control mAb is overlaid (dotted histograms).

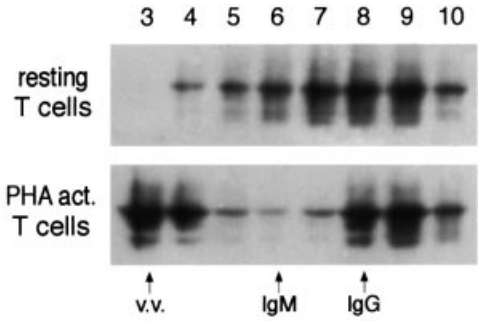

Fig. 8. Clustering of CD147 in PHA-activated T cells. Laurylmaltoside lysates of resting (top) or PHA-activated (bottom) T cells were fractionated by Sepharose 4B gel filtration, and the fractions were analyzed by SDS–PAGE and Western blotting. The fraction numbers are indicated on the top. The arrows indicate the fractions corresponding to elution maxima of large particles (fraction 3; void volume, v.v.), IgM (fraction 6) and IgG (fraction 8). The nitrocellulose blots were immunostained by using the MEM-M6/2 mAb. Only the relevant parts of the blots (~50 kDa) are shown.

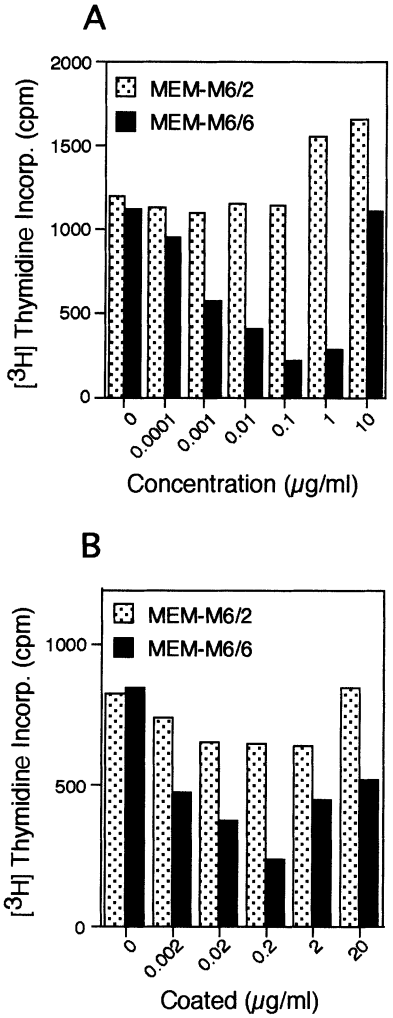

Fig. 9. Dose-dependent inhibition of OKT3-mediated T cell activation by CD147 mAb MEM-M6/6. T cells were stimulated with 1 μg/ml OKT3 in the presence of various concentrations of MEM-M6/6 in soluble form (A) or plate-bound form (B). mAb MEM-M6/2 was used as control.

binding model for explaining the activation-associated CD147 epitopes. Receptor-mediated functional effects are usually due to receptor dimerization or aggregation. Therefore, a prediction of this model was that either low-affinity mAb of suitable epitope specificity will display functional effects in a broad range of relatively high concentrations, or high-affinity mAb in a relatively narrow range of low, non-saturating concentrations, i.e. under the conditions when bivalent, rather than monovalent binding will be preferred. Thus, various concentrations of the CD147 mAb were added to T cells that were stimulated by sub-optimal concentrations of CD3 mAb OKT3 to allow detection of either stimulatory or inhibitory effects. Of the 15 CD147 mAb tested, mAb MEM-M6/6, recognizing a unique epitope, inhibited the OKT3-induced T cell proliferation up to 80% (Fig. 9A) when the mAb was added at a concentration of 0.1 μg/ml. Increasing and decreasing the concentration of MEM-M6/6 gradually abrogated the inhibitory effect. In agreement with the prediction of our model, the high-affinity mAb MEM-M6/6 exhibited the inhibitory effects optimally at relatively low (sub-saturating) concentrations. Under these conditions it bound presumably also monovalently because of the low CD147 density on resting T cells. However, upon T cell activation, CD147 molecules are up-regulated/clustered or may float in the proximity of the monovalently immobilized high-affinity mAb enabling bivalent binding and antigen dimerization. In contrast, at higher, saturating concentrations it bound mainly in a non-cross-linking, monovalent way. When we coated MEM-M6/6 on the surface of the culture well, similar inhibition curves were observed (Fig. 9B). This suggests that not merely multimerization but dimerization of CD147 in a specific orientation mediated by the unique MEM-M6/6 is the prerequisite to induce the inhibitory effect.

Discussion

In the present study we used a panel of newly established CD147 mAb in order to further characterize the CD147 molecule. While all of the mAb stained a number of hemopoietic and non-hemopoietic cell lines, a clear difference was seen with T lymphocytes. Some mAb stained resting T cells, whereas the majority of mAb bound only upon PHA activation. A conventional explanation of this result could be that activation-related epitope(s) are induced on the CD147 molecule. Given the potential functional significance of activation-restricted epitopes, e.g. the CD2R epitope seems to be linked to CD2-mediated T cell adhesion and activation (33), we tried to elucidate in molecular terms the nature of the apparent activation-associated CD147 epitopes. Now we provide evidence that binding of the 'restricted' CD147 mAb to activated T lymphocytes is not due to *de novo* exposure or expression of specific epitopes but rather it is determined by mAb affinity and antigen density. No correlation was found between the binding characteristics of the mAb to the resting versus activated T cells and the epitopes; however, those mAb with a relatively high affinity, i.e. $K_A > 7\times10^9$ M^{-1} bound to resting and activated T cells, mAb with a K_A between 7×10^9 and 2.25×10^8 M^{-1} stained PHA-activated T cells only, and the extremely low-affinity mAb 132 ($K_A = 2.19\times10^8$ M^{-1}) stained neither resting nor activated T cells under standard conditions. A plausible explanation of this correlation was that the high-affinity mAb can avidly and in a stable fashion bind monovalently to the CD147 antigen which is expressed on the resting T cell surface at a relatively low density. On the other hand, stable binding of the low-affinity mAb was expected to require bivalent binding, i.e. simultaneously with both binding sites of the IgG molecule. If the surface density of the antigen is too low, such bivalent interactions are unlikely, resulting in the loss of the low-affinity mAb during the washing steps and, therefore, in the lack of immunostaining of the cells. The low-affinity mAb can therefore stably bind to the cell surface either if the surface antigen density is sufficiently increased and/or if the antigen is unevenly distributed (clustered) on the cell surface so that a bivalent binding can occur in the areas of local clustering. Both these conditions appear to be met after T cell activation by PHA (Figs 2 and 8).

This model based on monovalent versus bivalent binding was supported by using monomeric and dimeric recombinant

forms of CD147. Soluble monomeric recombinant forms of CD147 could only be captured by the high-affinity mAb. The similarly constructed and produced dimeric forms of CD147 were bound by both the high-affinity mAb and the lower-affinity mAb that stained activated T cells (Fig. 7). In summary, these results strongly indicate that binding of the activation-dependent mAb to PHA blasts is not caused by expression of certain 'restricted' neoepitopes on the activated T cells but is due to a combination of increased antigen density (and/or clustering) and low mAb affinity. It is likely that some other formerly described cases of 'restricted' epitopes of cell surface molecules detected by specific mAb, e.g. the lymphocyte activation-associated Blast-1 epitope of the CD48 molecule (35), or the leukocyte subset-restricted CD99R epitopes of the broadly expressed CD99 molecule (36), may be explained in a similar way. Furthermore, CD2R has been shown to be restricted to clustered CD2 molecules which suggests that in addition to the proposed conformational alteration of CD2 (33), also the affinity of CD2R mAb may be critical for the definition of this epitope.

It is tempting to speculate that such low-affinity mAb can be valuable reagents specifically targeting clustered (or at least dimerized) subsets of cell surface molecules that may be functionally quite distinct from the monomeric subsets of the same molecules. One such interesting recently described example may be the dimerized subset of MHC class II molecules ('super-dimers') on the surface of antigen-presenting cells which can be of key importance for regulation of antigen presentation to T cells (37,38); it has been recently shown that a clustered subset of MHC class II molecules, possibly related to the 'super-dimers', is specifically recognized by low-affinity mAb that are assigned as CDw78 (39). In contrast to conventional MHC class II, the clustered MHC class II subset becomes associated with the cytoskeleton upon ligation with CDw78 mAb and is able to transduce signals (39).

Receptor dimerization is known to be an essential mechanism of signaling initiation via receptor tyrosine kinases or receptors associated with cytoplasmic tyrosine kinases (40). Here we provide evidence that also CD147 may require dimerization for initiation of a signaling function. We found one high-affinity mAb of unique epitope specificity, MEM-M6/6, that inhibited anti-CD3-induced T cell activation (Fig. 9). This mAb exerted its optimal T cell inhibitory effect at a relatively low concentration. No functional effect was seen at high concentrations and at extremely low concentration of the mAb (Fig. 9A). We explain this parabolic dose–response curve by a concentration-dependent monovalent versus bivalent binding mode of the mAb. At saturating concentrations it may, because of the excess of the mAb, preferentially bind monovalently and thus may be unable to dimerize the antigen. By increasing the antigen:mAb ratio through lowering the mAb concentration, bivalent binding and thus antigen dimerization becomes prevalent. Interestingly, aggregation of the cell surface CD147 by plastic-immobilized other CD147 mAb such as MEM-M6/2 is not sufficient to induce the functional effects and even the plastic-immobilized MEM-M6/6 works best at an optimal, relatively low concentration (Fig. 9B). This indicates that not just 'non-specific' aggregation of CD147, but rather oriented dimerization via the unique MEM-M6/6 mAb, is needed for initiation of T cell inhibition. The mechanism of this inhibitory activity of MEM-M6/6 mAb is at present unknown and is a subject of our further investigation.

In conclusion, we provide evidence that the existence of apparent T cell activation-dependent epitopes of the CD147 molecule can be explained at the molecular level by combined effects of mAb affinity and antigen density and/or clustering. This phenomenon should also be considered in other cases of restricted epitopes of other cell surface molecules. Moreover, our results, although so far based on a rather artificial, mAb-based system, suggest that CD147 is involved in regulation of the T cell response. These data lay ground for future identification of a possible natural ligand of CD147 and better defining of the physiological function of this molecule in the immune system.

Acknowledgements

We would like to thank Dr Brian Seed for the generous gift of the CD2Rg plasmid and Cornelia Hansmann for excellent technical assistance. This work was supported by a program project grant from the Austrian Science Foundation. The work of the Prague laboratory is supported in part by an International Research Scholar's Award from the Howard Hughes Medical Institute to V. H.

Abbreviations

dhfr$^-$	dihydrofolate reductase deficient
EMMPRIN	extracellular matrix metalloproteinase inducer
HBS	HEPES-buffered saline
H–ST	hinge–StrepTag
MFI	mean fluorescence intensity
PBMC	peripheral blood mononuclear cells
PHA	phytohemagglutinin
Rg	receptor globulin
RU	resonance units
ST	StrepTag

References

1 Stockinger, H., Ebel, T., Hansmann, C., Koch, C., Majdic, O., Prager, E., Patel, D. D., Fox, D. A., Horejsı, V., Sagawa, K. and Shen, D.-C. 1997. CD147 (neurothelin/basigin) workshop panel report. In Kishimoto, T., Kikutani, H., von dem Borne, A. E. G. K., Goyert, S. M., Mason, D. Y., Miyasaka, M., Moretta, L., Okumura, K., Shaw, S., Springer, T. A., Sugamura, K. and Zola, H., eds, *Leucocyte Typing VI*, p. 760. Garland Publishing, New York.

2 Kasinrerk, W., Fiebiger, E., Stefanova, I., Baumruker, T., Knapp, W. and Stockinger, H. 1992. Human leukocyte activation antigen M6, a member of the Ig superfamily, is the species homologue of rat OX-47, mouse basigin, and chicken HT7 molecule. *J. Immunol.* 149:847.

3 Biswas, C., Zhang, Y., DeCastro, R., Guo, H., Nakamura, T., Kataoka, H. and Nabeshima, K. 1995. The human tumor cell-derived collagenase stimulatory factor (renamed EMMPRIN) is a member of the immunoglobulin superfamily. *Cancer Res.* 55:434.

4 Miyauchi, T., Masuzawa, Y. and Muramatsu, T. 1991. The basigin group of the immunoglobulin superfamily: complete conservation of a segment in and around transmembrane domains of human and mouse basigin and chicken HT7 antigen. *J. Biochem.* 110:770.

5 Fossum, S., Mallett, S. and Barclay, A. N. 1991. The MRC OX-47 antigen is a member of the immunoglobulin superfamily with an unusual transmembrane sequence. *Eur. J. Immunol.* 21:671.

6 Nehme, C. L., Cesario, M. M., Myles, D. G., Koppel, D. E. and Bartles, J. R. 1993. Breaching the diffusion barrier that compartmentalizes the transmembrane glycoprotein CE9 to the posterior-tail plasma membrane domain of the rat spermatozoon. *J. Cell Biol.* 120:687.

7 Cesario, M. M. and Bartles, J. R. 1994. Compartmentalization,

processing and redistribution of the plasma membrane protein CE9 on rodent spermatozoa. *J. Cell Sci.* 107:561.
8 Seulberger, H., Lottspeich, F. and Risau, W. 1990. The inducible blood–brain barrier specific molecule HT7 is a novel immunoglobulin-like cell surface glycoprotein. *EMBO J.* 9:2151.
9 Schlosshauer, B. and Herzog, K. H. 1990. Neurothelin: an inducible cell surface glycoprotein of blood–brain barrier-specific endothelial cells and distinct neurons. *J. Cell Biol.* 110:1261.
10 Fadool, J. M. and Linser, P. J. 1993. 5A11 antigen is a cell recognition molecule which is involved in neuronal–glial interactions in avian neural retina. *Dev. Dyn.* 196:252.
11 Altruda, F., Cervella, P., Gaeta, M. L., Daniele, A., Giancotti, F., Tarone, G., Stefanuto, G. and Silengo, L. 1989. Cloning of cDNA for a novel mouse membrane glycoprotein (gp42): shared identity to histo-compatibility antigens, immunoglobulins and neural-cell adhesion molecules. *Gene* 85:445.
12 Miyauchi, T., Kanekura, T., Yamaoka, A., Ozawa, M., Miyazawa, S. and Muramatsu, T. 1989. Basigin, a new, broadly distributed member of the immunoglobulin superfamily, has strong homology with both the immunoglobulin V domain and the β-chain of major histocompatibility complex class II antigen. *J. Biochem.* 107:316.
13 Schuster, V. L., Lu, R., Kanai, N., Bao, Y., Rosenberg, S., Prie, D., Ronco, P. and Jennings, M. L. 1996. Cloning of the rabbit homologue of mouse 'basigin' and rat 'OX-47': kidney cell type-specific expression, and regulation in collecting duct cells. *Biochem. Biophys. Acta* 1311:13.
14 Kirsch, A. H., Diaz, L. A., Jr, Bonish, B., Antony, P. A. and Fox, D. A. 1997. The pattern of expression of CD147/neurothelin during human T-cell ontogeny as defined by the monoclonal antibody 8D6. *Tissue Antigens* 50:147.
15 Muraoka, K., Nabeshima, K., Murayama, T., Biswas, C. and Koono, M. 1993. Enhanced expression of a tumor-cell-derived collagenase-stimulatory factor in urothelial carcinoma: its usefulness as a tumor marker for bladder cancers. *Int. J. Cancer* 55:19.
16 Rizzo, A., Aragona, E., Dino, O., Pisa, R., Vignola, M., Guddo, F., Albanese, M., Guerrera, D., Orlando, A., Simonetti, R., Raiata, F., Realmuto, A., Bonsignore, G., Pagliaro, L. and Malizia, G. 1997. CD147 worshop: expression of CD147 (neurothelin) in liver and lung cancer. In Kishimoto, T., Kikutani, H., von dem Borne, A. E. G. K., Goyert, S. M., Mason, D. Y., Miyasaka, M., Moretta, L., Okumura, K., Shaw, S., Springer, T. A., Sugamura, K. and Zola, H., eds, *Leucocyte Typing VI*, p. 763. Garland Publishing, New York.
17 Guo, H., Zucker, S., Gordon, M. K., Toole, B. P. and Biswas, C. 1997. Stimulation of matrix metalloproteinase production by recombinant extracellular matrix metalloproteinase inducer from transfected Chinese hamster ovary cells. *J. Biol. Chem.* 272:24.
18 Schiavone, E. M., Tortora, V., Armetta, I., Bontempo, P., Mosti, M. R., Pezone, L., Nola, E., Puca, G. A., Vacca, C. and Molinari, A. M. 1997. CD147 workshop: expression, modulation, and involvement in homotypic aggregation and adhesion to matrix of molecules recognized by monoclonal antibodies to CD147 on breast cancer cell lines. In Kishimoto, T., Kikutani, H., von dem Borne, A. E. G. K., Goyert, S. M., Mason, D. Y., Miyasaka, M., Moretta, L., Okumura, K., Shaw, S., Springer, T. A., Sugamura, K. and Zola, H., eds, *Leucocyte Typing VI*, p. 764. Garland Publishing, New York.
19 Berditchevski, F., Chang, S., Bodorova, J. and Hemler, M. E. 1997. Generation of monoclonal antibodies to integrin-associated proteins. *J. Biol. Chem.* 272:29174.
20 Kuno, N., Kadomatsu, K., Fan, Q. W., Hagihara, M., Senda, T., Mizutani, S. and Muramatsu, T. 1998. Female sterility in mice lacking the basigin gene, which encodes a transmembrane glycoprotein belonging to the immunoglobulin superfamily. *FEBS Lett.* 425:191.
21 Igakura, T., Kadomatsu, K., Kaname, T., Muramatsu, H., Fan, Q. W., Miyauchi, T., Toyama, Y., Kuno, N., Yuasa, S., Takahashi, M., Senda, T., Taguchi, O., Yamamura, K., Arimura, K. and Muramatsu, T. 1998. A null mutation in basigin, an immunoglobulin superfamily member, indicates its important roles in peri-implantation development and spermatogenesis. *Dev. Biol.* 194:152.
22 Igakura, T., Kadomatsu, K., Taguchi, O., Muramatsu, H., Kaname, T., Miyauchi, T., Yamamura, K. I., Arimura, K. and Muramatsu, T. 1996. Roles of basigin, a member of the immunoglobulin superfamily, in behavior as to an irritating odor, lymphocyte response, and blood–brain barrier. *Biochem. Biophys. Res. Commun.* 224:33.
23 Naruhashi, K., Kadomatsu, K., Igakura, T., Fan, Q. W., Kuno, N., Muramatsu, H., Miyauchi, T., Hasegawa, T., Itoh, A., Muramatsu, T. and Nabeshima, T. 1997. Abnormalities of sensory and memory functions in mice lacking *BsG* gene. *Biochem. Biophys. Res. Commun.* 236:733.
24 Aruffo, A., Stamenkovic, I., Melnick, M., Underhill, C. B. and Seed, B. 1990. CD44 is the principal cell surface receptor for hyaluronate. *Cell* 61:1303.
25 Subramani, S., Mulligan, R. and Berg, P. 1981. Expression of the mouse dihydrofolate reductase complementary deoxyribonucleic acid in simian virus 40 vectors. *Mol. Cell. Biol.* 1:854.
26 Chen, C. and Okayama, H. 1987. High-efficiency transformation of mammalian cells by plasmid DNA. *Mol. Cell. Biol.* 7:2745.
27 Schmidt, T. G. and Skerra, A. 1993. The random peptide library-assisted engineering of a C-terminal affinity peptide, useful for the detection and purification of a functional Ig Fv fragment. *Prot. Eng.* 6:109.
28 Prager, E., Sunder-Plassmann, R., Hansmann, C., Koch, C., Holter, W., Knapp, W. and Stockinger, H. 1996. Interaction of CD31 with a heterophilic counterreceptor involved in downregulation of human T cell responses. *J. Exp. Med.* 184:41.
29 Johnsson, B., Lofås, S. and Lindquist, G. 1991. Immobilization of proteins to a carboxymethyldextran-modified gold surface for biospecific interaction analysis in surface plasmon resonance sensors. *Anal. Biochem.* 198:268.
30 Cinek, T. and Horejsi, V. 1992. The nature of large noncovalent complexes containing glycosyl-phosphatidylinositol-anchored membrane glycoproteins and protein tyrosine kinases. *J. Immunol.* 149:2262.
31 Bauer, A., Huttinger, R., Staffler, G., Hansmann, C., Schmidt, W., Majdic, O., Knapp, W. and Stockinger, H. 1997. Analysis of the requirement for β2-microglobulin for expression and formation of human CD1 antigens. *Eur. J. Immunol.* 27:1366.
32 Majdic, O., Pickl, W. F., Kohl, P., Stockinger, H. and Knapp, W. 1997. CD147 workshop: reactivity and epitope mapping of CD147 monoclonal antibodies. In Kishimoto, T., Kikutani, H., von dem Borne, A. E. G. K., Goyert, S. M., Mason, D. Y., Miyasaka, M., Moretta, L., Okumura, K., Shaw, S., Springer, T. A., Sugamura, K. and Zola, H., eds, *Leucocyte Typing VI*, p. 765. Garland Publishing, New York.
33 Li, J., Smolyar, A., Sunder-Plassmann, R. and Reinherz, E. L. 1996. Ligand-induced conformational change within the CD2 ectodomain accompanies receptor clustering: implication for molecular lattice formation. *J. Mol. Biol.* 263:209.
34 Fadool, J. M. and Linser, P. J. 1996. Evidence for the formation of multimeric forms of the 5A11/HT7 antigen. *Biochem. Biophys. Res. Commun.* 229:280.
35 Korinek, V., Stefanova, I., Angelisova, P., Hilgert, I. and Horejsi, V. 1991. The human leucocyte antigen CD48 (MEM-102) is closely related to the activation marker Blast-1. *Immunogenetics.* 33:108.
36 Bernard, A. 1997. CD99 workshop panel report. In Kishimoto, T., Kikutani, H., von dem Borne, A. E. G. K., Goyert, S. M., Mason, D. Y., Miyasaka, M., Moretta, L., Okumura, K., Shaw, S., Springer, T. A., Sugamura, K. and Zola, H., eds, *Leucocyte Typing VI*, p. 75. Garland Publishing, New York.
37 Cherry, R. J., Wilson, K. M., Triantafilou, K., O'Toole, P., Morrison, I. E., Smith, P. R. and Fernandez, N. 1998. Detection of dimers of dimers of human leukocyte antigen (HLA)-DR on the surface of living cells by single-particle fluorescence imaging. *J. Cell Biol.* 140:71.
38 Tobes, R., Pareja, E., Nieto, A. and Martin, J. 1998. Two classes of MHC class II interactions with the TCR [letter]. *Immunol. Today* 19:192.
39 Rasmussen, A. M., Horejsi, V., Levy, F. O., Blomhoff, H. K., Smeland, E. B., Beiske, K., Michaelsen, T. E., Gaudernack, G. and Funderud, S. 1997. CDw78—a determinant on a major histocompatibility complex class II subpopulation that can be induced to associate with the cytoskeleton. *Eur. J. Immunol.* 27:3206.
40 Heldin, C. H. 1995. Dimerization of cell surface receptors in signal transduction. *Cell* 80:213.